High efficiency solar cells combining a perovskite and a silicon heterojunction solar cells via an optical splitting system

Cite as: Appl. Phys. Lett. **106**, 013506 (2015); https://doi.org/10.1063/1.4905177
Submitted: 05 October 2014 • Accepted: 12 December 2014 • Published Online: 09 January 2015

Hisashi Uzu, Mitsuru Ichikawa, Masashi Hino, et al.

High efficiency solar cells combining a perovskite and a silicon heterojunction solar cells via an optical splitting system

Hisashi Uzu,[1,a)] Mitsuru Ichikawa,[1] Masashi Hino,[1] Kunihiro Nakano,[1] Tomomi Meguro,[1] José Luis Hernández,[2] Hui-Seon Kim,[3] Nam-Gyu Park,[3,a)] and Kenji Yamamoto[1]
[1]*Kaneka Corporation, 5-1-1, Torikai-Nishi, Settsu, Osaka 566-0072, Japan*
[2]*Kaneka Belgium N.V., Nijverheidsstraat 16, 2260 Westerlo-Oevel, Belgium*
[3]*School of Chemical Engineering and Department of Energy Science, Sungkyunkwan University, 300 Cheoncheon-dong, Jangan-gu, Suwon 440-746, South Korea*

(Received 5 October 2014; accepted 12 December 2014; published online 9 January 2015)

We have applied an optical splitting system in order to achieve very high conversion efficiency for a full spectrum multi-junction solar cell. This system consists of multiple solar cells with different band gap optically coupled via an "optical splitter." An optical splitter is a multi-layered beam splitter with very high reflection in the shorter-wave-length range and very high transmission in the longer-wave-length range. By splitting the incident solar spectrum and distributing it to each solar cell, the solar energy can be managed more efficiently. We have fabricated optical splitters and used them with a wide-gap amorphous silicon (a-Si) solar cell or a $CH_3NH_3PbI_3$ perovskite solar cell as top cells, combined with mono-crystalline silicon heterojunction (HJ) solar cells as bottom cells. We have achieved with a 550 nm cutoff splitter an active area conversion efficiency of over 25% using a-Si and HJ solar cells and 28% using perovskite and HJ solar cells. © *2015 AIP Publishing LLC*. [http://dx.doi.org/10.1063/1.4905177]

Conversion efficiencies about 25% have been reached for crystalline silicon solar cells[1] bringing the single-junction silicon solar cells closer to their theoretical limit of ~30% efficiency.[2] Multi-stack tandem solar cells can increase conversion efficiency beyond this limit.[3–5] However, optical management of tandem solar cells have some difficulties; therefore, we apply an optical splitting system.[6–12] Barnett *et al*. have reported the concept of an optical splitting system,[7–9] and we have applied this system to a crystalline silicon solar cell and a wide-band-gap thin film solar cell.

As seen in Fig. 1(a), the solar cells are set spatially separated and optically coupled via an "optical splitter" that divides the light beam at certain wavelength. Fig. 1(b) shows an example of the measurement setup. An optical splitter is a dichroic mirror that manages the spectral reflectance and transmittance directing the photons of different wavelengths to the most appropriate solar cell. The cells in the system are individually measured; therefore, the current for each cell does not need to be matched in contrast to standard tandem solar cells and they can be fabricated independently without any additional process constraints. This allows us to have a broader choice of materials and design options for the optical management of the systems.

In this paper, we present two types of optical splitting systems: one that consists of a wide-band-gap amorphous silicon (a-Si) solar cell (top) and a heterojunction (HJ) solar cell (bottom), and the other which consists of a $CH_3NH_3PbI_3$ perovskite solar cell (top) and a HJ solar cell (bottom).

In an optical splitting system, an optical splitter is positioned 45° with respect to both cells. The short wavelength radiation is reflected from the optical splitter to the top cell and the long wavelength radiation is transmitted to the bottom cell. The optical splitter is fabricated by sputter deposition of multi-layered dielectric oxides with high ($n \sim 1.9$–2.2) and low ($n \sim 1.5$) refractive indices on both sides of a glass substrate; this multilayer structure helps to reduce the reflection loss of the glass/air interface. We can control the optical properties, especially the cutoff wavelength by changing the number and thickness of the stacking layers. Kim *et al*. reported an optimum cutoff wavelength of around 600 nm using top and bottom cells with band gaps of 2.0 eV and 1.1 eV, respectively.[12] In this work, we have designed optical splitters that have a cutoff wavelength of 550 nm, 600 nm, and 640 nm. To optimize the optical splitter, we used commercial software.[13] As shown in Fig. 3, we fabricated optical splitters with very small optical losses, i.e., with very high reflectance and transmittance.

As a candidate for top cell, we used a wide-gap a-Si thin film solar cell with a size of $1 \times 1\,cm^2$. The a-Si cell consists of a standard pin structure deposited by plasma enhanced chemical vapor deposition (PECVD) on the glass substrate coated with a textured SnO_2. An intrinsic amorphous silicon (i:a-Si) layer was deposited increasing the hydrogen dilution in the plasma to get a wider band gap and thinner thickness than standard a-Si solar cells to increase V_{oc}. A transparent conducting oxide (TCO) and a Ag layers were deposited by sputtering on the rear side. In addition, a MgF_2 layer was deposited by electron beam deposition on the front side of the glass substrate as anti-reflection (AR) coating.

Another promising candidate for top cell is an organometallic halide perovskite ($CH_3NH_3PbX_3$, X = halogen)-based solar cell.[14] The merit of introducing perovskite solar cell in the optical splitting system is not only its high performance but also to the controllability of its band gap. Kulkarni *et al*. have reported band-gap tuning of the

a)Authors to whom correspondence should be addressed. Electronic addresses: Hisashi.Uzu@kaneka.co.jp and npark@skku.edu

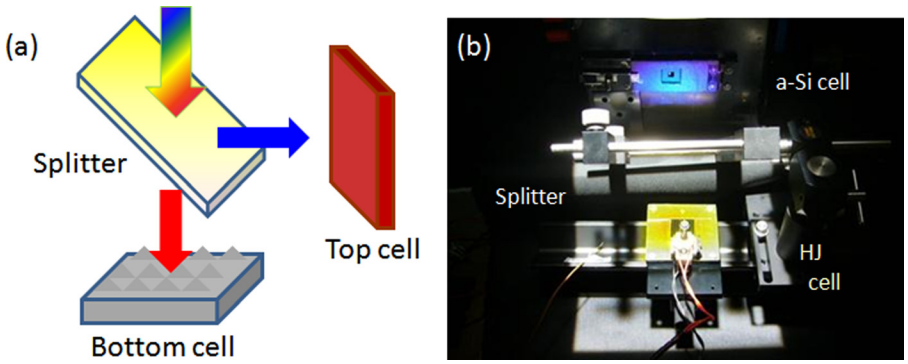

FIG. 1. (a) Schematic image of the optical splitting system and (b) measurement setup of an optical splitting system.

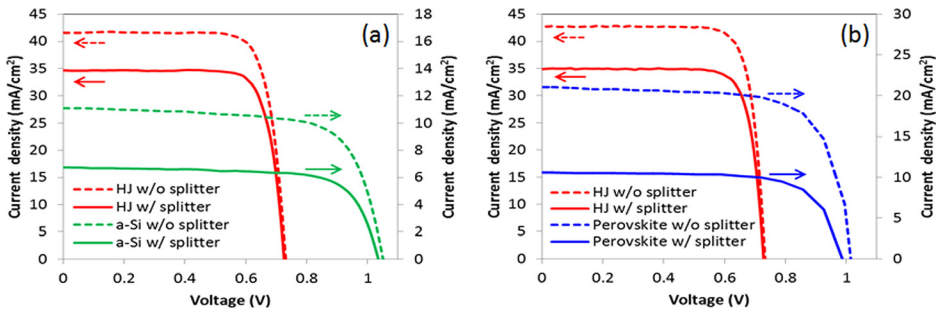

FIG. 2. Comparison between IV-curves of solar cells with and without splitter. (a) a-Si/HJ cell combinations. (b) Perovskite/HJ cell combination.

$CH_3NH_3Pb(I_{1-x}Br_x)_3$ perovskite cells by changing the ratio of iodine and bromine.[15] The optical band gap (E_g) of iodide-based $CH_3NH_3PbI_3$ perovskites is reported to be around 1.57 eV.[16] Solar cells fabricated with bromide-based $CH_3NH_3PbBr_3$ perovskites, $E_g = 2.3$ eV, is reported to have an open circuit voltage (V_{oc}) of 1.5 V with a chloride inclusion absorber, and a qV_{oc}/E_g ratio close to 0.7 has also been reported.[17] Meanwhile, perovskite solar cells still have some issues in reliability[18] comparing to commercialized solar cells such as crystalline silicon solar cells; therefore, the improvement of the perovskite device itself and also encapsulation techniques are required.

We have fabricated a superstrate type iodide-based $CH_3NH_3PbI_3$ perovskite cell.[19,20] In the perovskite cell, a compact TiO_2 blocking layer and a mesoporous TiO_2 film are deposited on a fluorine-doped tin oxide (FTO) coated glass substrate. A $CH_3NH_3PbI_3$ layer is prepared by one step method using an anti-solvent,[21] and a hole transport material (HTM) based on spiro-MeOTAD (Merck) is placed on the top of the perovskite layer. A thin Au layer is deposited by thermal evaporation on the HTM layer as a rear-side electrode. The dimension of the active area of the perovskite cell is 0.2 cm^2 (3×6.7 mm), and a mask with aperture of 2×2 mm^2 was used for the IV measurements to reduce measurement errors.

As for the bottom cell, we used mono-crystalline silicon HJ solar cells.[22,23] In a HJ cell structure, a randomly textured n-type Cz crystalline silicon (c-Si) wafer is passivated on both sides by an intrinsic a-Si thin layers, and a p-type and n-type a-Si layers are deposited on front and rear sides of the wafer. All a-Si layers are deposited using PECVD. A TCO layer is deposited on both sides and finally metal based grid electrode is formed on the front side, and a thin Ag layer is sputtered on the rear-side TCO. To reduce the reflection of the front surface, an MgF_2 layer is deposited on the front-side by electron beam deposition. A mask with an aperture of 2×2 cm^2 is used for HJ cell IV measurements.

IV measurements were performed under AM1.5G solar spectrum with a 550 nm cutoff splitter. For the calibration of the solar simulator, we used standard cells for thin film tandem solar cells. IV parameters for each cell are shown in Table I. J_{sc} and efficiency of HJ cell are active-area current and efficiency in which shadow loss of the grid electrodes on the front side surface is not taken into account. IV-curves for each cell are shown in Figs. 2(a) and 2(b). Because of the hysteresis behavior of perovskite cells,[24] we took an average of the IV curve obtained from two voltage sweep directions: V_{oc} to J_{sc} and J_{sc} to V_{oc}. Due to the use of the optical splitter, the efficiency of the a-Si solar cell is reduced from 8.3% to 5.1% and efficiency of the HJ solar cell goes down from

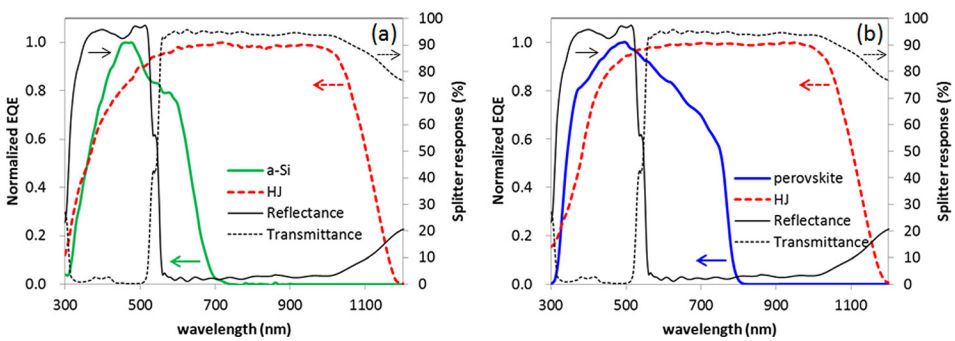

FIG. 3. Comparison between normalized EQEs of solar cells without splitter and optical properties of splitter. (a) a-Si and HJ cells. (b) Perovskite and HJ cells.

TABLE I. Output parameters of splitting system with and without a 550 nm cutoff splitter for an a-Si/HJ combination and a $CH_3NH_3PbI_3$ perovskite/HJ combination. J_{sc} and FF in the table denote short-circuit current density and fill factor, respectively. J_{sc} and Eff. of HJ cells represent active-area current and efficiency where shadow loss of the front grid electrodes is not taken into account.

a-Si/HJ combination

	a-Si (top)				HJ (bottom)				
Splitter	V_{oc} (V)	J_{sc} (mA/cm^2)	FF (%)	Eff. (%)	V_{oc} (V)	J_{sc} (mA/cm^2)	FF (%)	Eff. (%)	Total Eff. (%)
w/o	1.063	11.1	70.7	8.3	0.731	41.6	79.2	24.1	…
550 nm	1.045	6.7	72.6	5.1	0.725	34.7	79.1	19.9	25.0

$CH_3NH_3PbI_3$ perovskite/HJ combination

	Perovskite (top)				HJ (bottom)				
Splitter	V_{oc} (V)	J_{sc} (mA/cm^2)	FF (%)	Eff. (%)	V_{oc} (V)	J_{sc} (mA/cm^2)	FF (%)	Eff. (%)	Total Eff. (%)
w/o	1.015	21.1	71.6	15.3	0.733	42.7	80.5	25.2	…
550 nm	0.987	10.6	71.5	7.5	0.728	34.9	80.9	20.5	28.0

24.1% to 19.9%. In the case of the perovskite solar cell, the efficiency varies from 15.3% to 7.5% under the reflected light from the splitter. Using as top cell a perovskite solar cell instead of an a-Si top cell, a total conversion efficiency of 28.0% is obtained for the perovskite-HJ combined system. A comparison between the normalized external quantum efficiencies (EQEs) of solar cells without splitter and the optical properties of splitter are shown in Figs. 3(a) and 3(b). As seen in these figures, the a-Si and the perovskite cells contribute to the performance of the system in the shorter-wavelength range, while the HJ cell is active for the longer wavelengths. This way we can manage the incident solar spectrum by the optical splitter, and a high total efficiency is achieved.

We have examined the impact of the cutoff wavelength of the optical splitters in the perovskite-HJ system. As shown in Fig. 4, a decrease of the total efficiency is observed. This is mainly because the J_{sc} gain for the perovskite solar cell is suppressed by the loss of J_{sc} for the HJ cell.

To improve the total efficiency of the optical splitting system, increasing the V_{oc} of the top cell with appropriate optical management is crucial. As seen in Fig. 3(b), only the light below the cutoff wavelength contributes to the top cell current; therefore, a wider band gap top cell with higher V_{oc} than that of $CH_3NH_3PbI_3$ perovskite cell would keep the current when a 550 nm cutoff splitter is used. The increase of top cell V_{oc} keeping the other characteristics can enhance the total efficiency. A higher V_{oc} solar cell such as a $CH_3NH_3PbBr_3$ perovskite cell would improve the total efficiency of the optical splitting system.

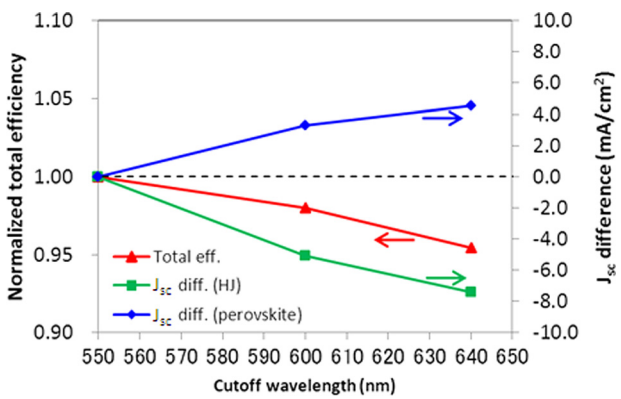

FIG. 4. Splitter cutoff wavelength dependences for a perovskite-HJ optical splitting system. Total efficiencies are normalized with respect to that of 550 nm cutoff splitter. Differences of J_{sc} from those of 550 nm cutoff splitter for perovskite and HJ cells are also shown.

In conclusion, we report an approach to achieve high conversion efficiency in a solar cell system by an optical splitting system incorporating top and bottom cell. A wide-gap amorphous thin film silicon solar cell and a $CH_3NH_3PbI_3$ perovskite solar cell are coupled via an optical splitter with a mono-crystalline silicon heterojunction solar cell. We have obtained active-area conversion efficiency of over 25% for the combination of a-Si and HJ solar cells, and 28% have been achieved for a perovskite and HJ optical splitting system. From this approach, the potential of optical splitting system towards high conversion efficiency is shown, and we believe that the improvement of the top cell will lead to conversion efficiencies over 30%.

The authors would like to acknowledge the financial support partially by the New Energy and Industrial Technology Development Organization (NEDO) under the Ministry of Economy, Trade and Industry (METI). This work was supported in part by the National Research Foundation of Korea (NRF) grants funded by the Ministry of Science, ICT & Future Planning (MSIP) of Korea under Contract No. NRF-2009-0092950.

[1]K. Masuko, M. Shigematsu, T. Hashiguchi, D. Fujishima, M. Kai, N. Yoshimura, T. Yamaguchi, Y. Ichihashi, T. Mishima, N. Matsubara, T. Yamanishi, T. Takahama, M. Taguchi, E. Maruyama, and S. Okamoto, IEEE J. Photovoltaics **4**(6), 1433–1435 (2014).
[2]W. Shockley and H. J. Queisser, J. Appl. Phys. **32**, 510 (1961).
[3]K. Yamamoto, A. Nakajima, M. Yoshimi, T. Sawada, S. Fukuda, T. Suezaki, M. Ichikawa, Y. Koi, M. Goto, T. Meguro, T. Matsuda, T. Sasaki, and Y. Tawada, in *Conference Record of the 2006 IEEE 4th World Conference on Photovoltaic Energy Conversion* (2006), p. 1489.
[4]M. Yamaguchi, Sol. Energy Mater. Sol. Cells **75**, 261–269 (2003).
[5]M. Yamaguchi, T. Takamoto, K. Araki, and N. Ekins.-Daukes, Sol. Energy **79**, 78–85 (2005).

[6]A. G. Imenes and D. R. Mills, Sol. Energy Mater. Sol. Cells **84**, 19–69 (2004).
[7]A. Barnett, D. Kirkpatrick, C. Honsberg, D. Moore, M. Wanlass, K. Emery, R. Schwartz, D. Carlson, S. Bowden, D. Aiken, A. Gray, S. Kurtz, L. Kazmerski, T. Moriarty, M. Steiner, J. Gray, T. Davenport, R. Buelow, L. Takacs, N. Shatz, J. Bortz, O. Jani, K. Goossen, F. Kiamilev, A. Doolittle, I. Ferguson, B. Unger, G. Schmidt, E. Christensen, and D. Salzman, paper presented at the 22nd European Photovoltaic Solar Energy Conference Milan, Italy, 3 September 2007.
[8]A. Barnett, X. Wang, N. Waite, P. Murcia, C. Honsberg, D. Kirkpatrick, D. Laubacher, F. Kiamilev, K. Goossen, M. Wanlass, M. Steiner, R. Schwartz, J. Gray, A. Gray, P. Sharps, K. Emery, and L. Kazmerski, paper presented at the 33rd IEEE Photovoltaic Specialists Conference (PVSC 33), San Diego, CA, USA, 20 May 2008.
[9]A. Barnett, D. Kirkpatrick, C. Honsberg, D. Moore, M. Wanlass, K. Emery, R. Schwartz, D. Carlson, S. Bowden, D. Aiken, A. Gray, S. Kurtz, L. Kazmerski, M. Steiner, J. Gray, T. Davenport, R. Buelow, L. Takacs, N. Shatz, J. Bortz, O. Jani, K. Goossen, F. Kiamilev, A. Doolittle, I. Ferguson, B. Unger, G. Schmidt, E. Christensen, and D. Salzman, Prog. Photovoltaics: Res. Appl. **17**, 75–83 (2009).
[10]J. D. McCambridge, M. A. Steiner, B. L. Unger, K. A. Emery, E. L. Christensen, M. W. Wanlass, A. L. Gray, L. Takacs, R. Buelow, T. A. McCollum, J. W. Ashmead, G. R. Schmidt, A. W. Haas, J. R. Wilcox, J. V. Meter, J. L. Gray, D. T. Moore, A. M. Barnett, and R. J. Schwartz, Prog. Photovoltaics: Res. Appl. **19**, 352–360 (2011).
[11]K. Yamamoto, paper presented at the 9th Workshop on the Future Direction of Photovoltaics, Tokyo, 7–8 March 2013.
[12]S. Kim, S. Kasashima, P. Sichanugrist, T. Kobayashi, T. Nakada, and M. Konagai, Sol. Energy Mater. Solar Cells **119**, 214–218 (2013).
[13]"The Essential Macleod" (version 9.4, 2012) developed by Thin Film Center, Inc.
[14]H.-S. Kim, C.-R. Lee, J.-H. Im, K.-B. Lee, T. Moehl, A. Marchioro, S.-J. Moon, R. Humphry-Baker, J.-H. Yum, J. E. Moser, M. Grätzel, and N.-G. Park, Sci. Rep. **2**, 591 (2012).
[15]S. A. Kulkarni, T. Baikie, P. P. Boix, N. Yantara, N. Mathews, and S. Mhaisalkarab, J. Mater. Chem. A **2**, 9221–9225 (2014).
[16]J. H. Noh, S. H. Im, J. H. Heo, T. N. Mandal, and S. I. Seok, Nano Lett. **13**, 1764–1769 (2013).
[17]W. Edri, S. Kirmayer, M. Kulbak, G. Hodes, and D. Cahen, J. Phys. Chem. Lett. **5**, 429–433 (2014).
[18]M. Grätzel, Nat. Mater. **13**, 838–842 (2014).
[19]J.-H. Im, C.-R. Lee, J.-W. Lee, S.-W. Park, and N.-G. Park, Nanoscale **3**, 4088–4093 (2011).
[20]J.-H. Im, H.-S. Kim, and N.-G. Park, APL Mater. **2**, 081510 (2014).
[21]N. J. Jeon, J. H. Noh, Y. C. Kim, W. S. Yang, S. Ryu, and S. I. Seok, Nat. Mater. **13**, 897–903 (2014).
[22]J. L. Hernández, D. Adachi, K. Yoshikawa, D. Schroos, E. V. Assche, A. Feltrin, N. Valckx, N. Menou, J. Poortmans, M. Yoshimi, T. Uto, H. Uzu, M. Hino, H. Kawasaki, M. Kanematsu, K. Nakano, R. Mishima, T. Kuchiyama, G. Koizumi, C. Allebé, T. Terashita, M. Hiraishi, N. Nakanishi, and K. Yamamoto, in *Proceedings of the 27th European Photovoltaic Solar Energy Conference and Exhibition* (2012), p. 655.
[23]J. L. Hernández, D. Adachi, D. Schroos, N. Valckx, N. Menou, T. Uto, M. Hino, M. Kanematsu, H. Kawasaki, R. Mishima, K. Nakano, H. Uzu, T. Terashita, K. Yoshikawa, T. Kuchiyama, M. Hiraishi, N. Nakanishi, M. Yoshimi, and K. Yamamoto, in *Proceedings of the 28th European Photovoltaic Solar Energy Conference and Exhibition* (2013), p. 741.
[24]H.-S. Kim and N.-G. Park, J. Phys. Chem. Lett. **5**, 2927–2934 (2014).